

Measurements of partial cross sections and autoionization in the photoionization of helium to $\text{He}^+(N=2)$

Pamela R. Woodruff*

Synchrotron Radiation Center, University of Wisconsin, Stoughton, Wisconsin 53589

James A. R. Samson

Behlen Laboratory of Physics, University of Nebraska, Lincoln, Nebraska 68588

(Received 10 July 1981)

We have measured the partial cross sections for ionizing neutral helium to He^+ in the $2s$ and $2p$ levels from threshold to 130 eV. Near threshold the data favor the close-coupling calculations of Jacobs and Burke rather than the many-body calculations of Chang, in contrast to the total $N=2$ cross section. We have also made a detailed study of the autoionizing resonances leading to the $N=3$, $N=4$, and $N=5$ thresholds. We present resonance parameters for the $N=3$ series. The energies of the resonances agree well with calculated and experimental values, but the widths show substantial disagreement with calculations.

I. INTRODUCTION

The importance of two-electron transitions in the photoionization of atoms and molecules is well established. Theoretical methods for dealing with them are still under development, although there have been some encouraging results for double ionization processes in the rare gases.¹ A firm theoretical basis of understanding will give a good handle on the more difficult problem of low-energy electron-impact excitation and ionization. In order to test existing theory, and in the hope of stimulating further developments, we have made a detailed study of the simultaneous ionization and excitation of helium, one of the simplest two-electron systems.

We have previously² reported measurements of the total photoionization cross section for the process:



The data are in good agreement with the recent many-body calculations of Chang.³ A more sensitive test of theory is to measure the partial cross sections for leaving the helium ion in either the $2s$ or $2p$ level. An earlier calculation,⁴ using relatively simple final-state wave functions, predicted that the final state would be almost entirely in the $2s$ level. However, both the close-coupling calculations of Jacobs and Burke⁵ and the calculations of Chang³ predict a substantial contribution from the

$2p$ level. The two calculations give values of the cross section for producing $\text{He}^+(2s)$ which agree well with each other at energies greater than 100 eV. Below 100 eV the values diverge considerably. We have made measurements of the cross section from threshold to 130 eV. The only previous experimental data of relevance are angular distribution measurements⁶ of the $N=2$ photoelectrons. These measurements were made at energies greater than 100 eV and do not directly measure the $2s:2p$ ratio. However, they do indicate a significant contribution from the $2p$ level.

Further insight into two-electron processes can be gained from looking at the autoionizing levels. Our earlier data showed evidence of strong interactions with autoionizing series leading to higher excited levels of He^+ . We have now scanned this region with far better resolution and so are able to identify many more lines and perform line-shape analyses on the stronger lines. Previous experimental studies^{7,8} of these resonances have been limited to their appearance in the total absorption cross section, where they are very weak. There are many theoretical calculations on the resonances using a variety of methods. Oberoi⁹ and Chung¹⁰ used Feshbach formalism; Herrick and Sinanoğlu¹¹ carried out configuration-interaction calculations using group theoretical methods to predict the mixing coefficients; Senaschenko and Wague¹² used a diagonalization approximation, and, finally, Ho^{13,14} used the complex rotation method. The approach

of Herrick and Sinanoğlu, and the hyperspherical coordinate approach of Macek,¹⁵ which was used on the $N=2$ resonances, also allow the relative strengths of the various possible series to be predicted. The predictions are borne out by experiment⁷ below the $N=2$ threshold where only three series are possible. For higher thresholds, the number of possible series rapidly increases, offering a more stringent test of the theories.

II. THE PARTIAL CROSS SECTIONS

A. Experimental

The $N=2$ levels of He^+ were detected by monitoring the 304-Å fluorescence resulting from their decay to the ground state of the ion. The incident photon range extended from 60 to 130 eV. In order to measure the $2p$ and $2s$ partial cross sections, it is necessary to find some means of monitoring the signal from the two levels separately. In principle this is straightforward. The $2p$ level decays with a lifetime of 10^{-10} s, while the $2s$ level is metastable with a lifetime of 2.2×10^{-3} s. Hence, in the absence of any perturbations, the fluorescence from the $2p$ level can be detected, while any ions in the $2s$ level will drift out of the line of sight of the detector before they decay. The application of a static electric field causes a mixing of the $2s$ and $2p$ levels, inducing the $2s$ level to decay by emission of a 304-Å photon, with a field-dependent lifetime¹⁶ T_D of

$$T_D = \frac{1.6 \times 10^{-2}}{U^2} \text{ s}, \quad (1)$$

where the field U is in V cm^{-1} . A field of greater than 500 V cm^{-1} is necessary to ensure that the $2s$ level will decay before the ion is accelerated out of the field of view. Hence the signal from the $\text{He}^+(2s)$ ions is the difference between the signal with the field applied and the field-free signal.

A major complication is the deexcitation of the $2s$ level through collisions with the background helium atoms. The measured¹⁷ deexcitation cross section is sufficiently large to ensure that, at the pressures needed to obtain a measurable signal, a significant fraction of the $2s$ levels will decay emitting a 304-Å photon, even in field-free conditions. It was therefore necessary to perform the experiment as a function of pressure, using pressures in the range $5 \times 10^{-4} - 8 \times 10^{-3}$ Torr.

The incident radiation was provided by synchrotron radiation from the Tantalus storage ring of

the University of Wisconsin. Most of the data were taken using a toroidal grating monochromator¹⁸ (TGM) set to give a bandpass of ~ 3 Å. Some additional data were taken with the Grasshopper grazing incidence monochromator at a bandpass of 2 Å. The incident radiation was monitored by means of a sodium salicylate covered window and a photomultiplier. The fluorescent radiation was detected by a proportional counter¹⁹ mounted at right angles to the incident beam. An aluminum counter was preferred over a stainless-steel one to minimize background problems associated with the decay of ^{53}Fe , which becomes activated during injection of the storage ring beam. The counter was operated with methane and was separated from the experimental chamber by a VYNS window.²⁰ Ultrahigh-purity helium was admitted to the chamber via a needle valve and the pressure was monitored by a differential capacitance manometer. A second VYNS window separated the helium from the high vacuum environment of the beamline. A 25-l s^{-1} ion pump was used on the low-pressure side of the window and further pressure differential was obtained by using a 150-mm long, 3-mm bore glass capillary between the ion pump and the exit of the monochromator.

Two parallel electrodes, 23 mm apart, supplied an electrostatic field across the interaction region. Their dimensions were chosen so that the field extended well beyond the field of view of the detector. The electrodes were coated with graphite to reduce reflections of both photons and electrons and baffles were placed in front of the proportional counter so that there was no direct line of sight to the electrode surfaces. The field was perpendicular to both the incident photon beam and the direction in which the fluorescence was detected.

Signal counting rates were in the range 3–30 s^{-1} with signal-to-background ratios of 1:1–20:1.

B. Analysis of the data

In the absence of an electrostatic field, all of the $2p$ levels decay, plus a fraction of the $2s$ levels. The number of $2s$ levels decaying depends on the number density of helium n_{He} , the collisional path length L' , and the collisional deexcitation cross section σ_{cd} . The signal detected S_0 is given by

$$S_0 = k [I_0 n_{\text{He}} L \sigma_{2p} + I_0 n_{\text{He}} L \sigma_{2s} (1 - \exp - n_{\text{He}} L' \sigma_{\text{cd}})], \quad (2)$$

where I_0 is the incident photon flux, L is the path

length for photoionization, σ_{2p} and σ_{2s} are the partial cross sections for producing He^+ in the $2p$ and $2s$ levels, and $n_{\text{He}}L\sigma_{2p} \ll 1$ and $n_{\text{He}}L\sigma_{2s} \ll 1$. The constant of proportionality k takes account of detector efficiency and geometrical factors.

With a sufficiently large field applied, all of the $2s$ levels will decay and the signal S_F will be given by

$$S_F = k [I_0 n_{\text{He}} L \sigma_{2p} + I_0 n_{\text{He}} L \sigma_{2s}] . \quad (3)$$

Equations (2) and (3) can be combined to give

$$\ln \frac{(S_F - S_0)}{S_F} = \ln \frac{(\sigma_{2s})}{(\sigma_{2s} + \sigma_{2p})} - n_{\text{He}} L' \sigma_{\text{cd}} . \quad (4)$$

Hence, plotting $\ln(S_F - S_0)/S_F$ against n_{He} (or, equivalently, against pressure) should give a straight line. At energies close to threshold this was found to be the case, but at higher energies the plot tends to a constant as the pressure increases. The reason for this behavior can be seen from a consideration of the effects of excitations to levels of He^+ with $N \geq 3$. With no field applied, a comparison with the equivalent lifetimes for hydrogen²¹ shows that the p levels will decay predominantly to the ground state. The radiation emitted will be of shorter wavelength than that from the $N=2$ decay and will be detected with greater efficiency owing to the transmission characteristics of the VYNS (Ref. 20) window. Excited s and d levels will predominantly cascade via the $2p$ level and so be detected with the same efficiency as the $N=2$ levels. When a field is applied, the most probable decay of the Stark-broadened s and d levels is directly to the ground state so that all of the levels with $N \geq 3$ will be detected with higher efficiency than the $N=2$ levels.

Hence, for energies above the $N=3$ threshold, Eq. (4) must be rewritten as

$$\ln \left[\frac{(S_F - S_0)}{S_F} - X \right] = \frac{\ln \sigma_{2s}}{Y} - n_{\text{He}} L' \sigma_{\text{cd}} , \quad (5)$$

with

$$X = \sum_{N \geq 3, l \neq p} \frac{\sigma_{Nl}(E_N - 1)}{Y} \quad (6)$$

and

$$Y = \sigma_{2p} + \sigma_{2s} + \sum_{N \geq 3} \sigma_N E_N , \quad (7)$$

where σ_{Nl} is the partial cross section for producing He^+ in the level (N, l) and E_N is the detection efficiency relative to that for 304 Å. $L' \sigma_{\text{cd}}$ can be

found from the measurements just above the $N=2$ threshold and with a knowledge of $(S_F - S_0)/S_F$ at several values of the pressure; a value for X can be found by a least-squares fit. Once X is known, σ_{2s}/Y can be found. Using the values of $(\sigma_{2s} + \sigma_{2p})$ measured previously,² together with values of σ_N from the data of Wuilleumier *et al.*²² and values of E_n from measurements of the transmission of the window used,²³ a value for σ_{2s} can finally be derived.

A second significant correction is for the anisotropy of the 304-Å fluorescence. The anisotropy of the fluorescence emitted when an electrostatic field is applied has been measured with great precision by Drake *et al.*²⁴ They also show that the anisotropy is approximately proportional to the ratio of the Lamb shift to the fine-structure splitting of the p levels. This ratio changes slowly with principal quantum number and so it has been assumed that the fluorescence from the higher excited states has the same anisotropy as that of the $N=2$ levels. Apart from a suggestion by Greene²⁵ that the fluorescence may be anisotropic within a fraction of an eV above threshold, there is no experimental or theoretical information on the anisotropy in the field-free situation. We have measured the fluorescence signal at 67 eV both parallel, S_{\parallel} , and perpendicular, S_{\perp} , to the major polarization axis of the incident radiation. The anisotropy, given by $(S_{\parallel} - S_{\perp})/(S_{\parallel} + S_{\perp})$ was found to be 0.00 ± 0.05 . The pressure for these measurements was quite high (0.05–0.3 Torr) and the data therefore include the presumably depolarizing effects of collisional deexcitation of the $2s$ levels. However, in the absence of any further information, we have assumed the field-free fluorescence to be isotropic at all energies. The correction increases the measured $2s$ cross section by up to 20%.

There are other mechanisms that could produce a spurious increase in fluorescence when a field is applied, such as electron impact excitation of the $N=2$ level from either the neutral atom or the ground state of the ion. At the pressures used there were too few electrons produced by photoionization to give a measurable signal. A more likely source would be electrons emitted from surfaces struck by the incident photon beam. The experiment was carefully aligned so that there was no direct path for the photon beam to any surface near the interaction region. However, as a check, measurements were made below the $N=2$ threshold. A small signal was found below the $N=2$ threshold which increased when the field was ap-

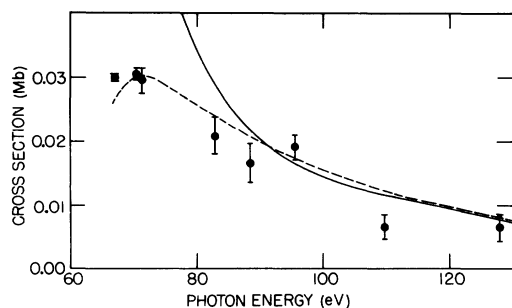


FIG. 1. The partial cross section for producing $\text{He}^+(2s)$ from neutral helium. \bullet : this work; —: Chang (Ref. 3); - - -: Jacobs and Burke (Ref. 5).

plied. On the Grasshopper monochromator the signal was about 5% of the signal measured just above threshold, while with the TGM the value was 10%. This suggested that the signal was due to second-order radiation, which is known to be a high proportion of the total flux from the TGM.¹⁸ To verify this assumption, the value of $(S_F - S_0)/S_F$ was measured with first-order radiation at an energy corresponding to the below-threshold second-order radiation. The value obtained agreed with that measured below threshold to well within the experimental errors. The signal measured below threshold was therefore used to correct the above-threshold values for second-order effects over the range where these are known to be a problem.

The plots of $\ln(S_F - S_0)/S_F$ against pressure for the measurements made near threshold gave a value of $L'\sigma_{cd}$ of $63 \pm 2 \text{ Torr}^{-1}$. Estimating the mean pathlength to be 5 mm gives a value for the collisional deexcitation cross section of $\approx 4 \times 10^{-15} \text{ cm}^2$. This compares reasonably well with the value of $5.2 \times 10^{-15} \text{ cm}^2$ measured by Prior and Wang¹⁷ for helium ions with a mean energy of 0.23 eV.

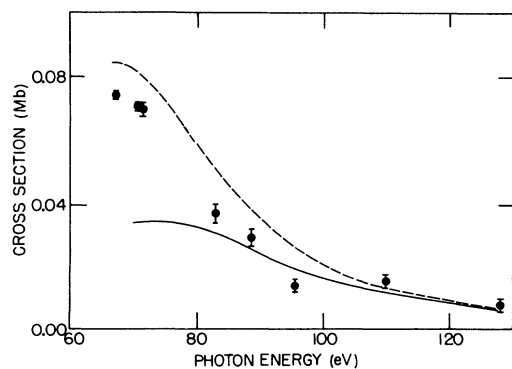


FIG. 2. The partial cross section for producing $\text{He}^+(2p)$ from neutral helium. \bullet : this work; —: Chang (Ref. 3); - - -: Jacobs and Burke (Ref. 5).

TABLE I. Absolute cross sections for $\text{He} + h\nu \rightarrow \text{He}^+(2s, 2p) + e^-$.

Energy (eV)	Cross section (10^{-21} cm^2)	
	2s	2p
67.0	29.9 ± 0.5	74.1 ± 0.5
70.1	30.6 ± 1.0	70.4 ± 1.0
71.3	29.5 ± 1.9	69.5 ± 1.9
82.7	20.9 ± 3.0	37.1 ± 3.0
88.6	16.6 ± 3.1	29.4 ± 3.1
95.4	19.1 ± 2.0	13.9 ± 2.0
109.7	6.5 ± 2.0	15.4 ± 2.0
127.8	6.0 ± 2.0	8.0 ± 2.0

C. Results and discussion

The measured photoionization cross sections for $\text{He}(1s^2) \rightarrow \text{He}^+(2s)$, $\text{He}^+(2p)$ are shown in Figs. 1 and 2. The numerical data are listed in Table I. The error bars represent random errors from counting statistics and uncertainties in finding values for the parameter X [see Eq. (5)]. Additional systematic errors come from uncertainties in the total cross section ($\sim 7\%$), uncertainties in the corrections for the higher excited states ($\sim 10\%$), and in the anisotropy correction ($\sim 10\%$), giving a probable systematic error of 12% below the $N=3$ threshold and 16% above it.

The data are compared with the calculated cross sections of Jacobs and Burke⁵ and Chang.³ For the 2s cross section (Fig. 1) above 85 eV, both theories lie approximately 10% higher than the data. The data for the 2p cross section (Fig. 2) in the same energy region agree reasonably well with both theories. At low energies the data clearly favor the close-coupling calculation of Ref. 5. This is a little unexpected in view of the excellent agreement between experiment and the calculation of Ref. 3 for the total cross section for the $N=2$ level, and serves to underline the value of measurements of the partial cross sections in comparing photoionization theories. The close-coupling calculation includes contributions from the $N=3$ pseudostates in the final-state wave function and so it appears that these have opposite effects in the 2s and 2p cross sections. It should be noted that the data points below 73 eV are inherently more accurate than the remaining points since there was no necessity to correct them for the effects of the higher excited states.

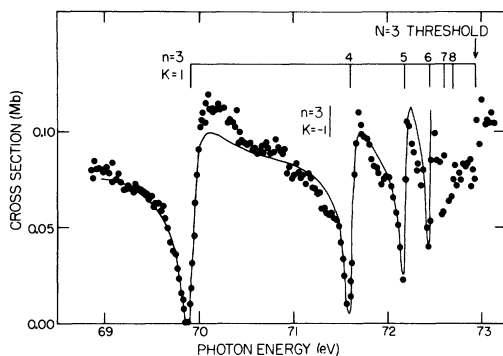


FIG. 3. The autoionizing region below the $N=3$ threshold. The full line is a fit to the data (see text).

III. AUTOIONIZATION

A. Experimental

The apparatus used was similar to that used to obtain the partial cross sections, the major difference being the absence of the electrodes. The helium pressure was generally about 0.2 Torr. From

the value of the product of the pathlength and the collisional deexcitation cross section obtained in the partial cross-section measurements, the percentage of $\text{He}^+(2s)$ states that will not decay with emission of a $304\text{-}\text{\AA}$ photon at this pressure is $2 \times 10^{-4}\%$. This is clearly negligible and hence the data to be presented reflect the effects of autoionization on the total $N=2$ cross section.

The experiment was performed using the Grasshopper grazing incidence monochromator set to give a bandpass of 0.08 \AA . The energy calibration of the monochromator has been established over a long period of time. As a check the Al $2p$ edge, which lies conveniently within the autoionizing region, was scanned and its position was found to agree with the established calibration. The data are the result of combining multiple scans of the autoionizing region. They were normalized to the photon flux and a small correction for second-order radiation was made which was derived from the signal measured below the $N=2$ threshold. Counting rates were typically in the range 10–20

TABLE II. Resonance parameters for the first four members of the 1_n series.

	Shore parameters ^a			Fano parameters ^b		
1_3	$E_0 = 69.917$	(± 0.012)	eV	$q = 0.48$	(± 0.09)	Mb
	$\Gamma = 0.178$	(± 0.012)	eV	$\sigma_a = 0.084$	(± 0.021)	
	$A = 0.081$	(± 0.014)	Mb	$\rho^2 = 0.98$	+ 0.02	
	$B = 0.065$	(± 0.008)	Mb		-0.26	
1_4	$E_0 = 71.601$	(± 0.018)	eV	$q = 0.47$	(± 0.10)	Mb
	$\Gamma = 0.096$	(± 0.015)	eV	$\sigma_a = 0.084$	(± 0.024)	
	$A = 0.079$	(± 0.017)	Mb	$\rho^2 = 0.98$	+ 0.02	
	$B = -0.066$	(± 0.010)	Mb		-0.29	
1_5	$E_0 = 72.181$	(± 0.015)	eV	$q = 0.62$	(± 0.14)	Mb
	$\Gamma = 0.067$	(± 0.015)	eV	$\sigma_a = 0.071$	(± 0.031)	
	$A = 0.088$	(± 0.021)	Mb	$\rho^2 = 0.83$	+ 0.17	
	$B = -0.044$	(± 0.012)	Mb		-0.37	
1_6	$E_0 = 72.453$	(± 0.011)	eV	$q = 0.49$	(± 0.16)	Mb
	$\Gamma = 0.038$	(± 0.015)	eV	$\sigma_a = 0.087$	(± 0.039)	
	$A = 0.085$	(± 0.028)	Mb	$\rho^2 = 1.00$	+ 0.00	
	$B = -0.066$	(± 0.016)	Mb		-0.46	
	$C = 0.086$	(± 0.007)	Mb			

Systematic errors are the same for each member and are $E_0 \pm 0.009$ eV, $\Gamma \pm 0.008$ eV, $A \pm 0.016$ Mb, $B \pm 0.015$ Mb, $C \pm 0.014$ Mb

^aReference 28.

^bReference 30.

s^{-1} . The data were placed on an absolute scale by normalizing to the previous measurements² away from the autoionizing region.

B. Results and discussion

To facilitate identification of the various resonances, the notation of Herrick and Sinanoğlu¹¹ will be used. Thus, the resonances are described by N , the ionization threshold to which the series converges; n , the principal quantum number of the series member; and K and T , integer quantum numbers which characterize the configurationally mixed, doubly excited states. All the doubly excited states that can be reached by photoionization of ground-state helium have $T=1$ and hence the states below a particular threshold are designated by K_n .

The cross section for the autoionizing region below the $N=3$ threshold is shown in Fig. 3. In addition to the scatter of the experimental points, there is a systematic error in the absolute cross section of about 7%. One series can be seen which clearly interacts strongly with the $N=2$ continua. This is identified as the 1_n series, which is equivalent to the “+” series of Refs. 26, 15, and 10, where it was predicted to be the only channel which should be strongly excited. A similar phenomenon was observed in H^- .²⁷ The solid line in Fig. 3 represents a least-squares fit to the four lowest resonances using the parametrization given by Shore²⁸

$$\sigma = C(E) + \sum_k \frac{(E - E_{0k})A_k \Gamma_k / 2 + B_k (\Gamma_k / 2)^2}{(E - E_{0k})^2 + (\Gamma_k / 2)^2} \quad (8)$$

Equation (8) is based on the assumption that the resonances do not interact with each other. To obtain the line shown, the monochromator response function, which was a Gaussian of FWHM of 0.08 Å, was first deconvoluted from the data using the technique described by Allen and Grimm.²⁹ A least-squares fitting routine was then used to find the parameters, and finally the derived line shapes were reconvoluted with the monochromator function. The parameters are given in Table II together with the derived Fano parameters q, σ_a and the correlation coefficient ρ^2 . The background $C(E)$ was assumed to be constant for the whole series. Within the experimental errors, values for A and B , and hence for the Fano parameters, since

$q = [B \pm (A^2 + B^2)^{1/2}] / A$, $\sigma_a = A / (2q)$, and $\rho^2 = \sigma_a / C$, are remarkably constant throughout the first four members of the series. The widths of the three higher members scale as $1/n^3$ within the errors. Both of these observations are in agreement with the analysis of Fano and Cooper.³⁰ From Table II, $q < 1$, and so the excess oscillator strength for the series, and hence the contribution of the $N=3$ levels at threshold, is negative and is estimated to be -0.01 Mb. However, there is clearly a rise in the cross section at the $N=3$ threshold. Assuming the $3s:3p$ ratio to be the same as that measured for the $2s$ and $2p$ levels, the $N=3$ threshold cross section is approximately 0.01 Mb.

Of the four other possible autoionizing series, only one other, the -1_n , is predicted to be allowed by the selection rules of Ref. 11. There is evidence of weak structure around 71.30 eV which can be identified as the first member of the -1_n series. The estimated width of 70 meV agrees well with that given in Refs. 11 and 12 though is rather larger than that given in Ref. 13. Higher members of this series are predicted to overlap with the 1_n series members.

The positions and widths of the resonances are compared in Table III with other experimental and theoretical values. The 1_3 resonance has been studied in detail in the total absorption cross section by Dhez and Ederer,⁸ where it appears to have a very weak effect. Subtracting the cross section for the $N=2$ level from the total reveals the shape of the resonance in the $N=1$ cross section. The absolute change in the magnitude of the $N=1$ cross section is almost equal to that of the $N=2$ cross section. The resonance has a q of about -2.7 , i.e., the maximum is on the low-energy side of the resonance energy. This is very close to the q values found for the resonances below the $N=2$ threshold⁷ and shows that, as predicted by Ref. 30, the value of q for a particular continuum is fairly independent of the threshold to which the series converges. The weak appearance of the 1_3 resonance in the total cross section is therefore the result of the almost complete cancellation that occurs in the sum of the $N=1$ and $N=2$ cross sections. The resonance energies in the two experiments are in excellent agreement. The width found in the present experiment is somewhat greater than that of Ref. 8 but there is agreement within the total errors (random plus systematic). The other experimental values in Table II are from the work of Madden and Codling.⁷ Taking note of the fact that

TABLE III. Autoionization energies and widths below the $N = 3$ threshold. Values are expressed in eV.

Identification	This work	Other experiment	Ref. 9	Ref. 10	Ref. 11	Other theory
1_3 E	69.917 (± 0.012)	69.919 ^a (± 0.007) 69.94 ^b (± 0.04)	69.872	69.842	69.89	69.917 ^c 69.8727 ^d (± 0.0014) 69.85 ^e 69.91 ^f
Γ	0.178 (± 0.012)	0.132 ^b (± 0.014)			0.151	0.204 ^c 0.191 ^d 0.149 ^f
1_4 E	71.601 (± 0.018)	71.66 ^b (± 0.01)	71.628	71.602	71.66	71.67 ^f
Γ	0.096 (± 0.015)				0.0476	0.0463 ^f
1_5 E	72.181 (± 0.015)	72.20 ^b (± 0.01)	72.186	72.164	72.20	
Γ	0.067 (± 0.015)				0.0171	
1_6 E	72.453 (± 0.011)	72.47 ^b (± 0.01)	72.454	72.436	72.49	
Γ	0.038 (± 0.015)					
1_7 E	72.59 (± 0.01)	72.61 ^b (± 0.01)	72.590	72.603		
1_8 E	72.67 (± 0.01)	72.70 ^b (± 0.01)	72.675			
-1_3 E	71.30 (± 0.04)		71.316	71.283	71.45	71.309 ^d (± 0.013) 71.46 ^f
Γ	≈ 0.07				0.0677	0.038 ^d (± 0.004) 0.0669 ^f

^aReference 8.^bReference 7. Energies were measured at the maxima of the resonances.^cReference 31.^dReference 13.^eReference 32.^fReference 12.

the energies were measured at the peak of absorption and are therefore expected to be higher than the resonance energies, the general agreement is good. The various theoretical values for the energies are also in generally good agreement, particularly for the higher series members. The comparison for the widths is not as good. For the 1_3 resonance, the theoretical values lie either too high or too low. For the 1_4 and 1_5 resonances, the calculated widths are lower than the experimental widths by factors of 2 and 4, respectively.

The resonances converging on the $N = 4$ and $N = 5$ thresholds are shown in Fig. 4. Above the $N = 3$ threshold, there are contributions to the fluorescence signal from the higher excited states through cascades, and direct transitions to the ground state. The structure seen is, therefore, the result of autoionization to all levels except the $N = 1$. Again, a single, strong series is seen leading

to each of the $N = 4$ and $N = 5$ thresholds. The series are identified as the 2_n and 3_n series, respectively. The resonances appear to become more windowlike as the higher thresholds are reached. The slight dip in the cross section between the 2_4

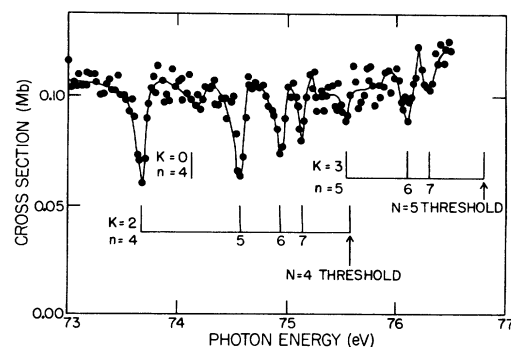


FIG. 4. The autoionizing regions below the $N = 4$ and $N = 5$ thresholds.

TABLE IV. Autoionization energies below the $N=4$ and $N=5$ thresholds of He^+ . Values are expressed in eV.

Identification	This work ^a	Ref. 7 ^b	Ref. 9	Ref. 11	Ref. 14
2 ₄	73.66 (± 0.03)	73.76 (± 0.02)	73.702	73.70	73.712
2 ₅	74.57 (± 0.03)	74.64 (± 0.02)	74.633	74.63	
2 ₆	74.93 (± 0.03)	75.00 (± 0.02)	74.992	74.99	
2 ₇	75.14 (± 0.03)				
0 ₄	74.15 (± 0.04)		74.213	74.21	74.141
3 ₅	75.54 (± 0.04)			75.55	
3 ₆	76.10 (± 0.03)			76.10	
3 ₇	76.30 (± 0.03)				

^aEnergies measured at the minimum of each resonance.

^bEnergies measured at the maximum of each resonance.

and 2₅ resonances is tentatively identified as the first member of the 0_{*n*} series. Its relative broadness in comparison with the 2₄ resonance is in agreement with theory.^{11,13} Also in agreement with theory¹¹ is the observation that the first member of the 3_{*n*} series, which converges to the $N=5$ threshold, lies marginally below the $N=4$ threshold. The positions of the resonances, measured at the minima of the cross section, are given in Table IV along with other experimental and theoretical values. As before, the values of Ref. 7 were measured at the maxima in the total absorption cross section. The agreement with both previous experiment and theory is reasonably good.

IV. CONCLUSIONS

The measurements made for the total and partial cross sections for the $N=2$ level show that the theoretical situation is somewhat ambiguous. The total cross section agrees very well with the calculation of Chang,³ while the partial cross sections favor the Jacobs and Burke⁵ calculations. Further work, both experimental and theoretical, is needed

to clarify the discrepancy. Some of the difficulties encountered in the present experiment could be eliminated by using microwave power at the Lamb shift frequency (14.045 GHz) to induce decay of the 2s level without affecting the higher excited levels.

For the autoionizing resonances, the various theories predict the positions and relative strengths of the series fairly well. However, the widths, which are far more sensitive to the accuracy of the continuum wave functions, do not agree well with the data.

ACKNOWLEDGMENTS

We should like to thank E. W. Plummer of the University of Pennsylvania for the use of the toroidal grating monochromator and J. E. Manson for loaning the proportional counter. This work was supported by the National Science Foundation under Contract No. DMR 8020164 and by the National Aeronautics and Space administration under Grant No. NGR 28-002-021.

*Present address: Department of Natural Philosophy, University of Aberdeen, Aberdeen AB9 1UE Scotland.

¹See, e.g., S. L. Carter and H. P. Kelly, Phys. Rev. A **16**, 1525 (1977).

²P. R. Woodruff and J. A. R. Samson, Phys. Rev. Lett. **45**, 110 (1980).

³T. N. Chang, J. Phys. B **13**, L551 (1980).

⁴R. L. Brown, Phys. Rev. A **1**, 341 (1970).

⁵V. L. Jacobs and P. G. Burke, J. Phys. B **5**, L67 (1972).

⁶M. O. Krause and F. J. Wuilleumier, J. Phys. B **5**,

L143 (1972).

⁷R. P. Madden and K. Codling, Astrophys. J. **141**, 364 (1965).

⁸P. Dhez and D. L. Ederer, J. Phys. B **6**, L59 (1973).

⁹R. S. Oberoi, J. Phys. B **5**, 1120 (1972).

¹⁰K. T. Chung, Phys. Rev. A **6**, 1809 (1972).

¹¹D. R. Herrick and O. Sinanoğlu, Phys. Rev. A **11**, 97 (1975).

¹²V. S. Senashenko and A. Wague, J. Phys. B **12**, L269 (1979).

- ¹³Y. K. Ho, *J. Phys. B* **12**, 387 (1979).
¹⁴Y. K. Ho, *Phys. Lett.* **79A**, 44 (1980).
¹⁵J. Macek, *J. Phys. B* **1**, 831 (1968).
¹⁶W. E. Lamb and M. Skinner, *Phys. Rev.* **78**, 539 (1950).
¹⁷M. H. Prior and E. C. Wang, *Phys. Rev. A* **9**, 2383 (1974).
¹⁸B. P. Tonner, *Nucl. Instr. and Meth.* **172**, 133 (1980).
¹⁹Gas Flow Photon Counter, J. E. Manson Co., P. O. Box 1288, 238 Holden Wood Rd., Concord, Mass. 19742.
²⁰J. E. Manson, *Appl. Opt.* **12**, 1394 (1973).
²¹W. L. Wiese, M. W. Smith, and B. M. Glennon, *Atomic Transition Probabilities*, Vol. 1, NSRDS-NBS 4 (Nat. Bur. Stand., Washington, D. C., 1966).
²²F. J. Wuilleumier, *Electronic and Atomic Collisions*, edited by N. Oda and K. Takayanagi (North Holland, Amsterdam, 1980), p. 55.
²³T. Masuoka, private communication.
²⁴G. W. F. Drake, S. P. Goldman, and A. van Wijngaarden, *Phys. Rev. A* **20**, 1299 (1979).
²⁵C. H. Greene, *Phys. Rev. Lett.* **44**, 869 (1980).
²⁶J. W. Cooper, U. Fano, and F. Prats, *Phys. Rev. Lett.* **10**, 518 (1963).
²⁷M. E. Hamm, R. W. Hamm, J. Donahue, P. A. M. Gram, J. C. Pruett, M. A. Yates, R. D. Bolton, D. A. Clark, H. C. Bryant, C. A. Frost, and W. W. Smith, *Phys. Rev. Lett.* **43**, 1715 (1979).
²⁸B. W. Shore, *Phys. Rev.* **171**, 43 (1968).
²⁹J. D. Allen and F. A. Grimm, *Chem. Phys. Lett.* **60**, 72 (1979).
³⁰U. Fano and J. W. Cooper, *Phys. Rev.* **137**, 1364 (1965).
³¹P. G. Burke and A. J. Taylor, *J. Phys. B* **2**, 44 (1969).
³²S. Ormonde, W. Whitaker, and L. Lipsky, *Phys. Rev. Lett.* **19**, 1161 (1967).